Supplementary for

Measurement Report: Distinct size dependence and diurnal variation of OA hygroscopicity, volatility, and CCN activity at a rural site in the Pearl River Delta (PRD) region, China

Mingfu Cai[1,2,3], Shan Huang[1,2*], Baoling Liang[4], Qibin Sun[4], Li Liu[5*], Bin Yuan[1,2], Min Shao[1,2], Weiwei Hu[6], Wei Chen[6], Qicong Song[1,2], Wei Li[1,2], Yuwen Peng[1,2], Zelong Wang[1,2], Duohong Chen[7], Haobo Tan[5], Hanbin Xu[4], Fei Li[5], Xuejiao Deng[5], Tao Deng[5], Jiaren Sun[3], and Jun Zhao[4,8,9]

[1] Institute for Environmental and Climate Research, Jinan University, Guangzhou, Guangdong 511443, China

[2] Guangdong-Hongkong-Macau Joint Laboratory of Collaborative Innovation for Environmental Quality, Guangzhou, Guangdong 511443, China

[3] Guangdong Province Engineering Laboratory for Air Pollution Control, Guangdong Provincial Key Laboratory of Water and Air Pollution Control, South China Institute of Environmental Sciences, MEE, Guangzhou, Guangdong 510655, China

[4] School of Atmospheric Sciences, Guangdong Province Key Laboratory for Climate Change and Natural Disaster Studies, and Institute of Earth Climate and Environment System, Sun Yat-sen University, Zhuhai, Guangdong 519082, China

[5] Institute of Tropical and Marine Meteorology of China Meteorological Administration, Guangzhou 510640, China

[6] State Key Laboratory of Organic Geochemistry and Guangdong Key Laboratory of Environmental Protection and Resources Utilization, Guangzhou Institute of Geochemistry, Chinese Academy of Sciences, Guangzhou 510640, China

[7] Guangdong Environmental Monitoring Center, Guangzhou 510308, China

[8] Southern Marine Science and Engineering Guangdong Laboratory (Zhuhai), Zhuhai, Guangdong 519082, China

[9] Guangdong Provincial Observation and Research Station for Climate Environment and Air Quality Change in the Pearl River Estuary, Guangzhou, Guangdong 510275, China

*Corresponding authors: Shan Huang (shanhuang_eci@jnu.edu.cn) and Li Liu (liul@gd121.cn)

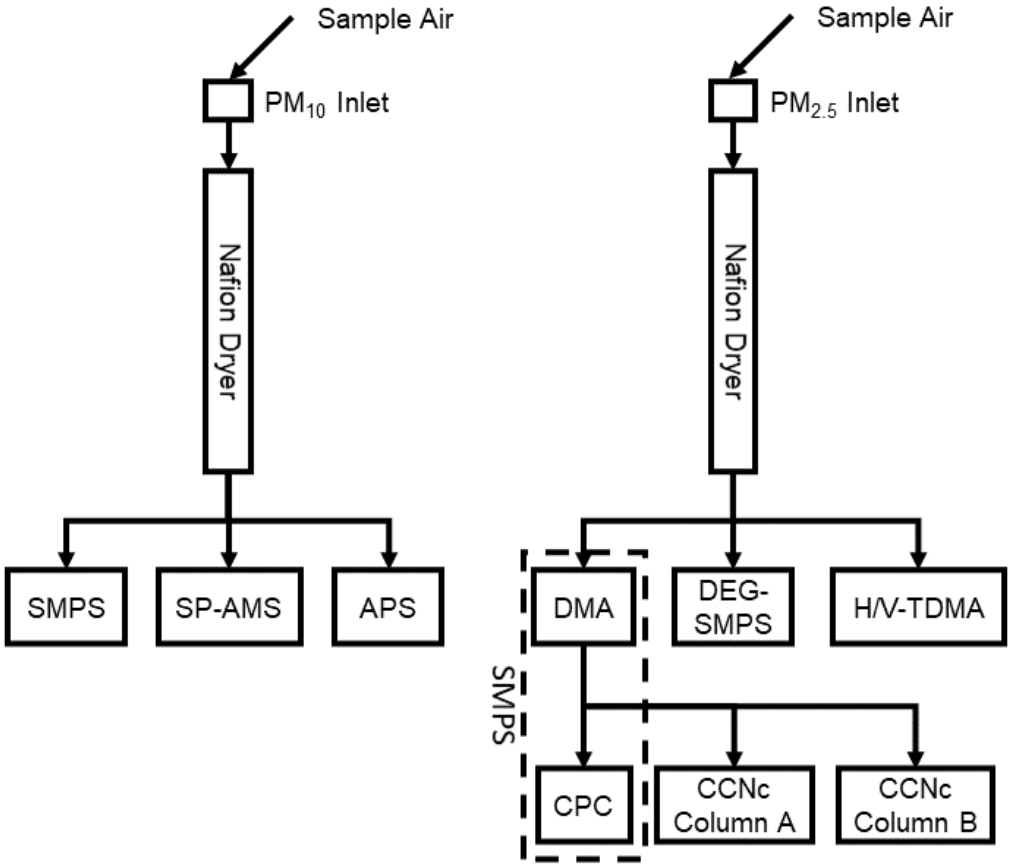

Figure S1. Schematic diagram of the experimental setup

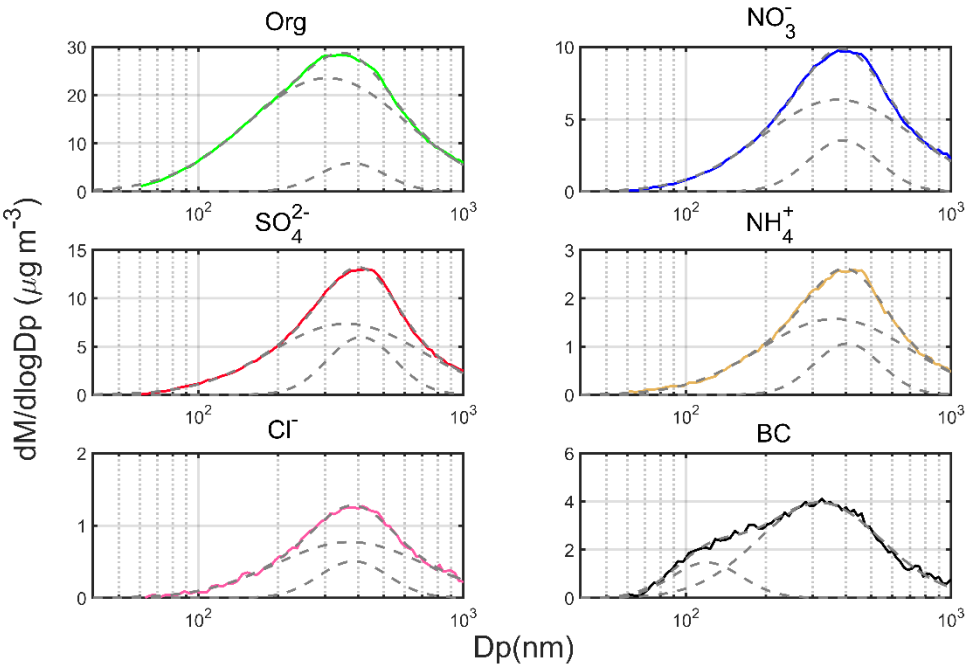

Figure S2. The average mass distribution of each species measured by the AMS, along with bimodal lognormal fitted modes (grey dash line).

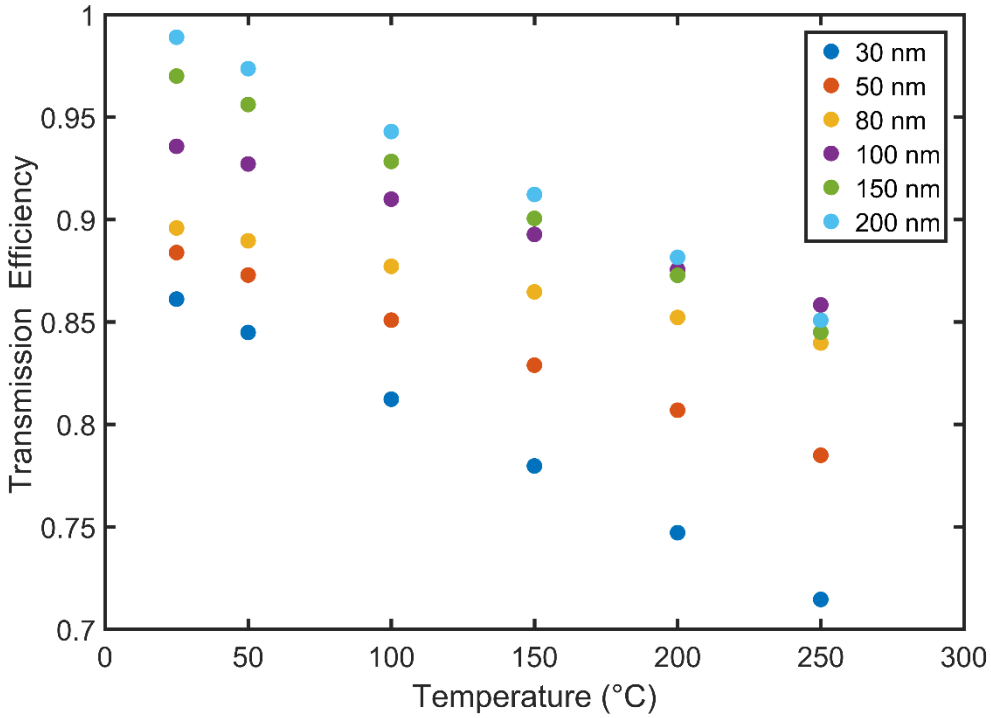

Figure S3. The transmission efficiency (η) of NaCl between DMA_1 and DMA_2 at different sizes and temperatures.

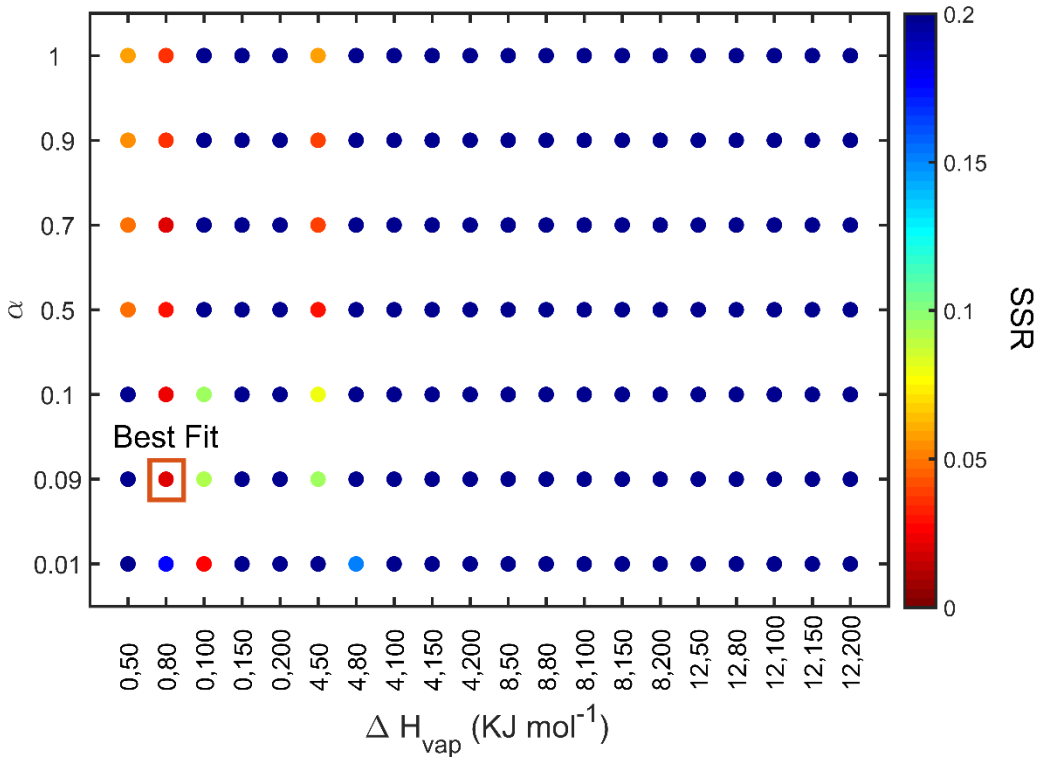

Figure S4. SSR values of different fitness of the campaign averaged MFR. The color code represents the value of SSR. The distribution of each species is solved based on different combinations of ΔH_{vap} of OA and α. The ΔH_{vap} is assumed to be as a function of $C_i^*(T_{ref})$, $\Delta H_{vap} = -a \cdot log_{10} C_i^*(T_{ref}) + b$, e.g., "0, 50" on the x axis suggests a=0 and b=50. A lower SSR suggests a better fit. The orange square represents the best fitting results.

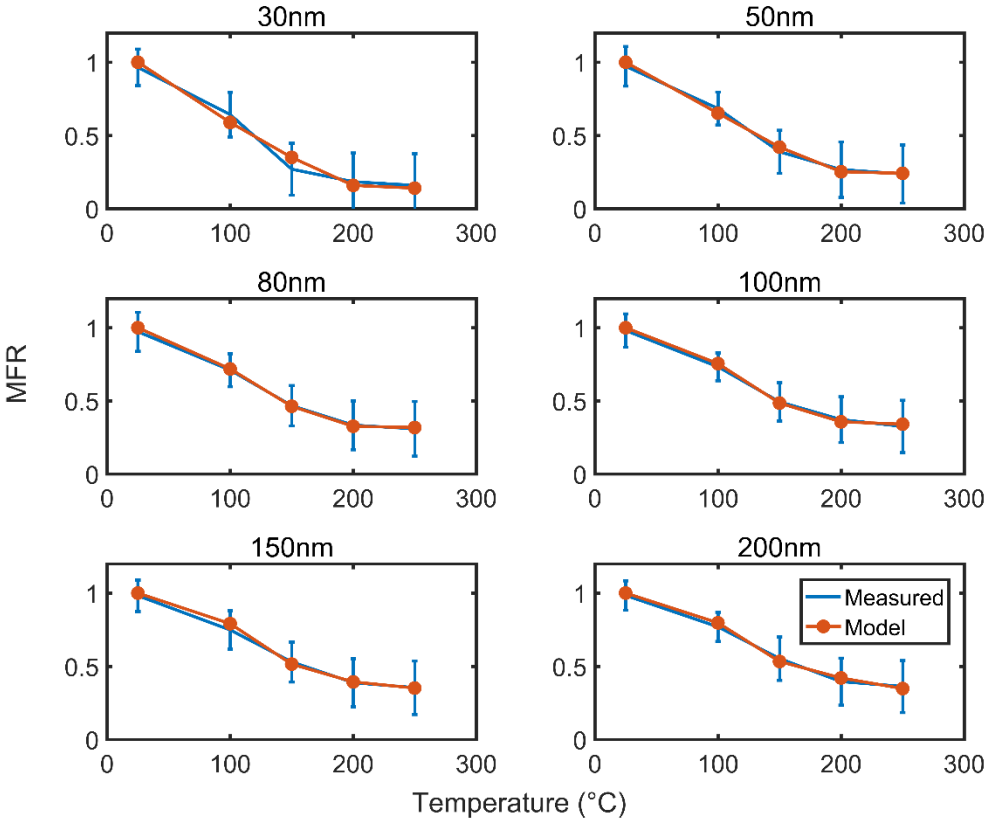

Figure S5. Measured (blue lines) and modeled (red lines) campaign average MFRs at six measured diameters (30, 50, 80, 100, 150, and 200 nm). The error bar of measured MFRs represents $\pm$ 1 standard deviation. ΔH_{vap}=80 kJ mol^{-1} and α=0.09 are adopted in the simulation.

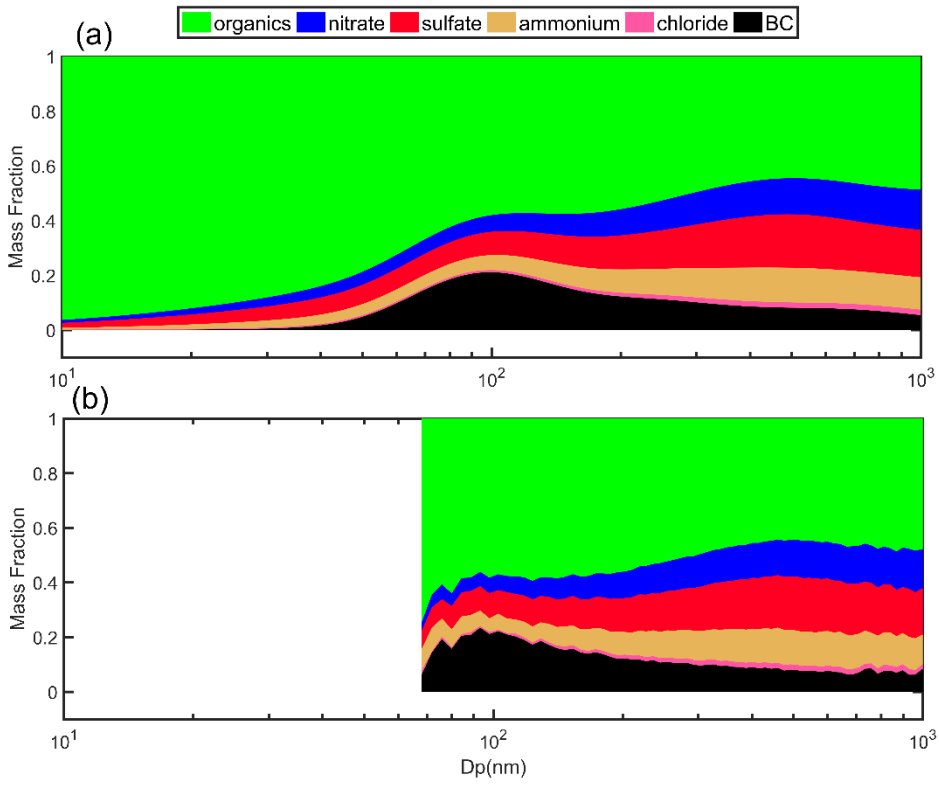

Figure S6. The average mass fraction of the size-resolved composition based on the lognormal fit (a) and measurement (b).

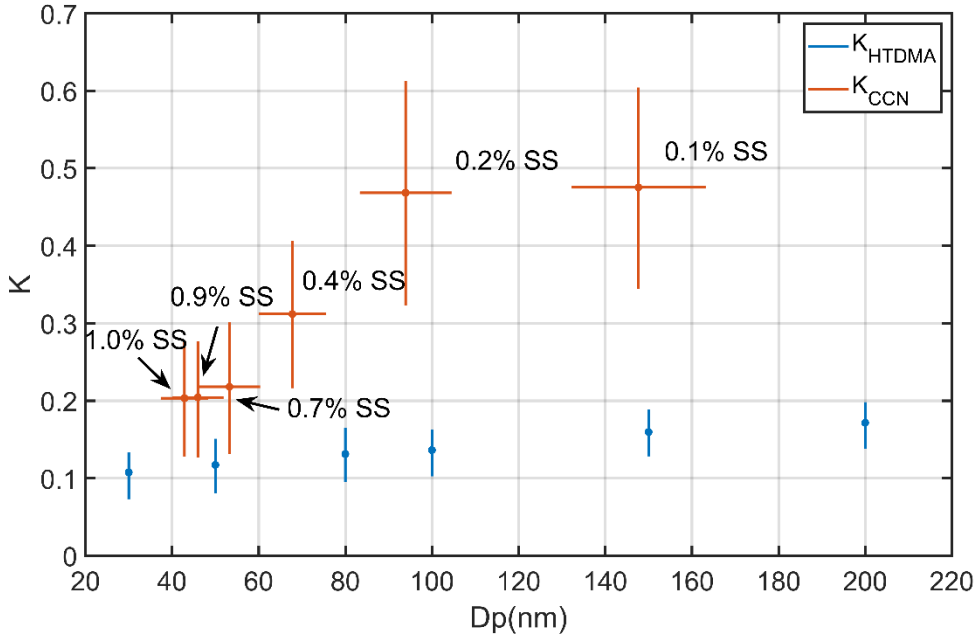

Figure. S7 The mean and standard deviation values of κ_{CCN} and κ_{HTDMA} during the campaign. The κ values were pointed against their corresponding mean D_{50} (κ_{CCN}) or selected diameter (κ_{HTDMA}). The dots represent the mean values, and the bars represent the one standard deviation.

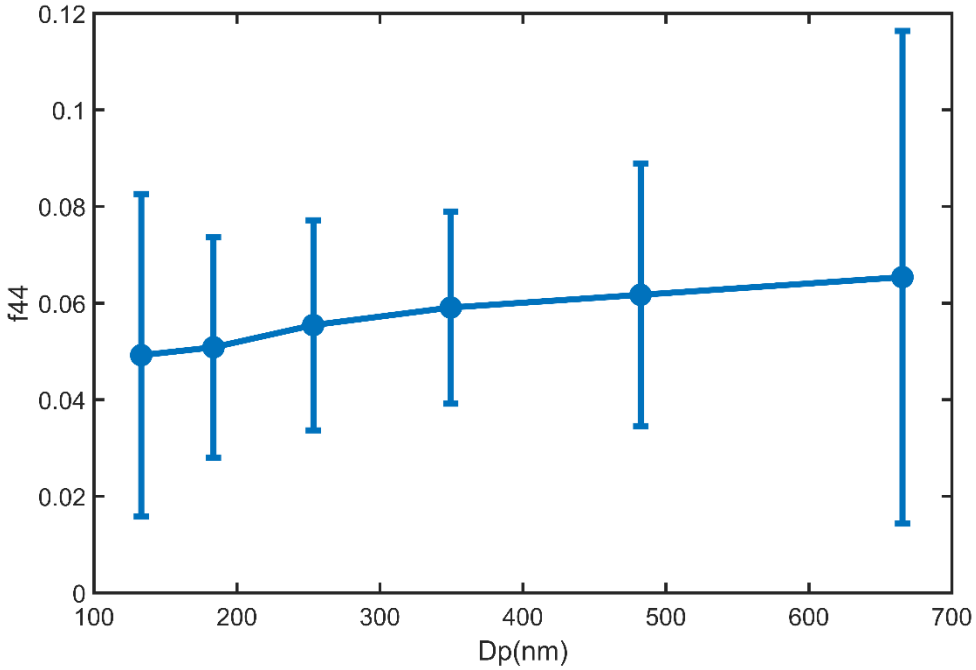

Figure S8. The campaign average size-resolved f44 with the upper and lower error bars.

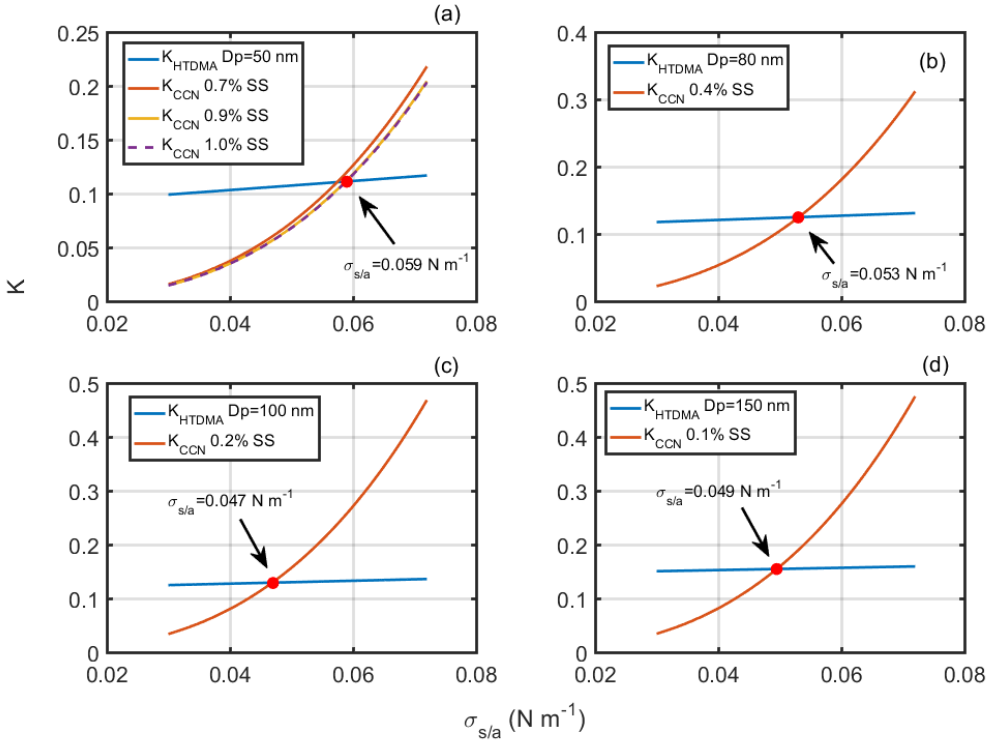

Figure S9. κ_{CCN} and κ_{HTDMA} at different assumed $\sigma_{s/a}$. κ_{HTDMA} at 50, 80, 100 and 150 nm is adopted to compared with κ_{CCN} at 0.7%, 0.9%, and 1.0% SS, 0.4% SS, 0.2% SS, and 0.1% SS, respectively. Red dot represents the intersection point of κ_{CCN} and κ_{HTDMA}.

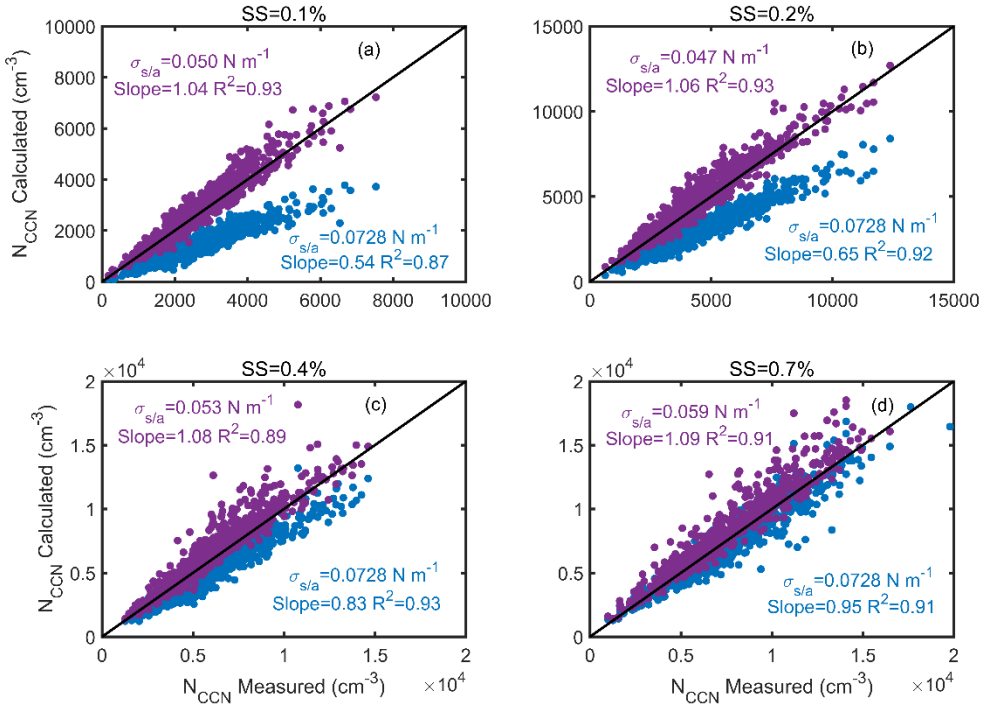

Figure S10. The predicted and measured N_{CCN} at 0.1%, 0.2%, 0.4%, and 0.7% SS based on the $\sigma_{s/a}$ value (0.0728 N m^{-1}) for pure water (bule dots) and reduced $\sigma_{s/a}$ values (purple dots). The reduced $\sigma_{s/a}$ values were set to be 0.049 N m^{-1} at 0.1% SS, 0.047 N m^{-1} at 0.2% SS, 0.053 N m^{-1} at 0.4% SS, and 0.059 N m^{-1} at 0.1% SS, respectively. The N_{CCN} at four SS was predicted based on fixed κ_{OA} scheme.